International Scholarly Research Network
ISRN Nanotechnology
Volume 2012, Article ID 416417, 7 pages
doi:10.5402/2012/416417

Research Article

The Electronic Properties of the Graphene and Carbon Nanotubes: *Ab Initio* Density Functional Theory Investigation

Erkan Tetik,[1] Faruk Karadağ,[1] Muharrem Karaaslan,[2] and İbrahim Çömez[1]

[1] *Physics Department, Faculty of Sciences and Letters, Çukurova University, 01330 Adana, Turkey*
[2] *Electrical and Electronic Engineering Department, Faculty of Engineering, Mustafa Kemal University, 31040 Hatay, Turkey*

Correspondence should be addressed to Erkan Tetik, etetik@student.cu.edu.tr

Received 20 December 2011; Accepted 13 February 2012

Academic Editors: A. Hu, C. Y. Park, and D. K. Sarker

We examined the graphene and carbon nanotubes in 5 groups according to their structural and electronic properties by using *ab initio* density functional theory: zigzag (metallic and semiconducting), chiral (metallic and semiconducting), and armchair (metallic). We studied the structural and electronic properties of the 3D supercell graphene and isolated SWCNTs. So, we reported comprehensively the graphene and SWCNTs that consist of zigzag (6, 0) and (7, 0), chiral (6, 2) and (6, 3), and armchair (7, 7). We obtained the energy band graphics, band gaps, charge density, and density of state for these structures. We compared the band structure and density of state of graphene and SWCNTs and examined the effect of rolling for nanotubes. Finally, we investigated the charge density that consists of the 2D contour lines and 3D surface in the XY plane.

1. Introduction

The physics of carbon nanotubes (CNTs) has evolved into a research field since their discovery [1]. The CNTs have been researched in a lot of forms from single-walled (SWCNT) and multiwalled (MWCNT) carbon nanotubes to array and bundle carbon nanotubes. A SWCNT can be described as a graphene sheet rolled into a cylindrical shape along a vector with the specified direction which is called chiral vector. SWCNTs can be characterized by the chiral vector $\vec{C}_h = n\vec{a}_1 + m\vec{a}_2$ (n, m are integers and $0 \leq |m| \leq n$). SWCNTs can be classified as armchair (n, n), zigzag $(n, 0)$, and chiral (n, m) nanotubes [2, 3]. The geometrical structure of SWCNTs can directly affect their electronic properties and other several characteristics like mechanical, thermal, and transport. Experimental studies and electronic band structure calculations [4, 5] indicate that the (n, m) indices determine the metallic and semiconducting behavior of SWCNTs. The semiconducting energy gap in the SWCNTs depends on the nanotube diameter [6]. Zigzag $(n, 0)$ SWCNTs shows the metallic characteristic when $n/3$ is an integer. Otherwise, they are semiconducting. When $\vec{C}_h$ rotates away from zigzag $(n, 0)$, chiral (n, m) SWCNTs are obtained. Chiral (n, m) SWCNTs show the metallic characteristic when $(2n + m)/3$ is an integer. Otherwise, they are semiconducting. Finally, when $\vec{C}_h$ rotates 30° relative to zigzag $(n, 0)$, armchair (n, n) SWCNTs are obtained and their n and m indices are equal. The armchair (n, n) SWCNTs are expected to show metallic characteristic [7].

The existence of SWCNTs has been confirmed experimentally through high-resolution transmission electron microscopy (TEM) [8] and scanning tunneling microscopy (STM) [9]. The electronic properties of SWCNTs have been studied by a lot of researchers since that time. For example, Minot et al. [10] who employed atomic force microscopy (AFM) reported the results that showed the band gap changes with the stretch of the CNT. Additionally, Dohn et al. [11] found that the conductance of MWCNTs varies as a function of the applied strain. Moreover, Tombler et al. [12] reported that the electrical properties of CNT vary with the tapping depth in AFM applications. Many simulation-based studies have been performed to show the potential to use the unique electronic properties of SWCNTs to develop nanoscale electronic devices. In recent years,

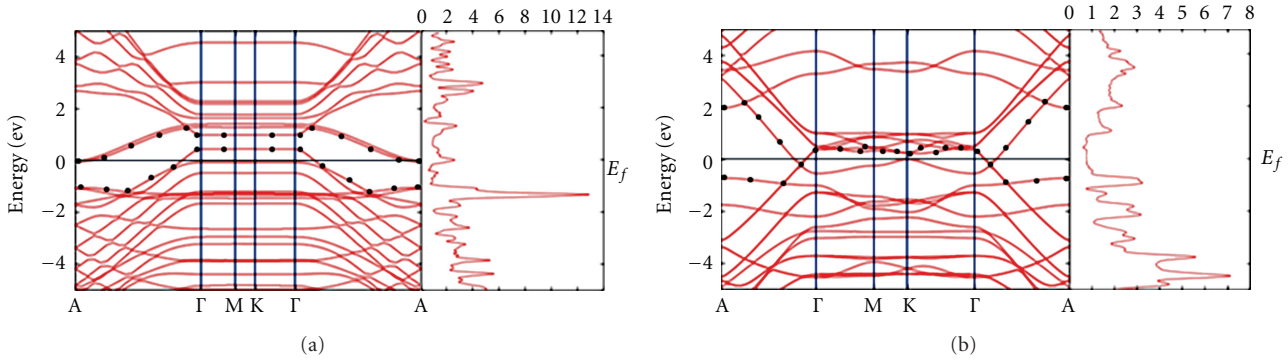

Figure 1: Electronic band structure and DOS of zigzag (6, 0) graphene (a) and nanotube (b).

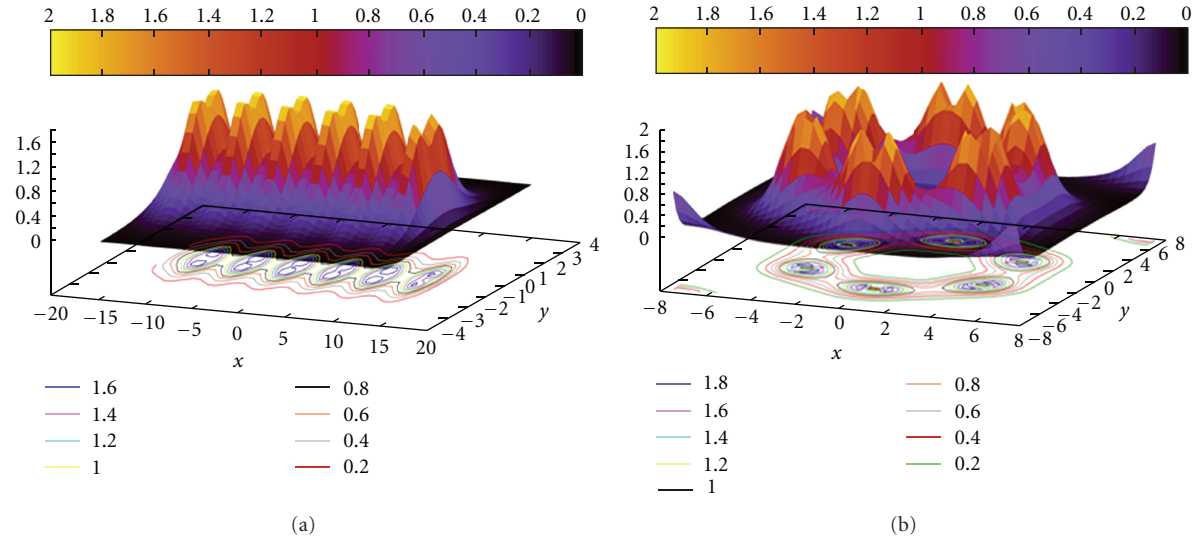

Figure 2: Charge density of the zigzag (6, 0) graphene (a) and nanotube (b).

molecular dynamic simulation-based programs have been used to investigate the electronic and mechanical properties of SWCNTs.

Here we reported on a detailed study of the electronic properties, density of state (DOS), and charge density of supercell graphene and isolated SWCNTs. We examined the carbon nanotubes in 5 groups according to their structures and electronic properties: zigzag (metallic and semiconducting), chiral (metallic and semiconducting), and armchair (metallic). We investigate the effects of rolling from graphene to nanotube and discuss the electronic properties of zigzag (6, 0) (24 atoms) and (7, 0) (28 atoms), chiral (6, 2) (104 atoms) and (6, 3) (84 atoms), and armchair (7, 7) (28 atoms) nanotubes. In Section 2 we describe the computational method used in this work. The electronic properties and charge density of graphene and isolated nanotubes are presented in Section 3. Finally, Section 4 summarizes our work and contains our conclusions.

2. The Material and Computational Methods

In our work we used two programs, the TubeGen code [13] and SIESTA *ab initio* package [14]. We relaxed the nanotubes by using the radius_conv, error_conv, and gamma_conv, which are parameters in the TubeGen code, and obtained the atomic position and the lattice parameters, which were used in the SIESTA input file.

The total energy and electronic structure calculations are performed via the first principles density functional theory, as implemented in the SIESTA. For the solution method we used the diagon, a parameter in the SIESTA. For the exchange and correlation terms, we used the local density approximation (LDA) parameterized by Perdew and Zunger [15] and nonlocal norm-conserving pseudo potentials [16]. For carbon atoms 1s state is the core state, while the 2s and 2p states form the valence states. The valence electrons were described by localized pseudo atomic orbitals with

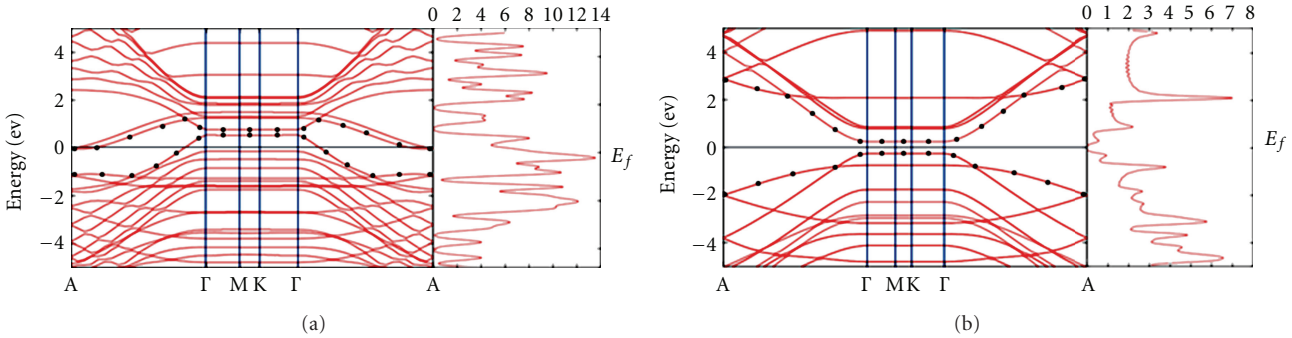

Figure 3: Electronic band structure and DOS of zigzag (7, 0) graphene (a) and nanotube (b).

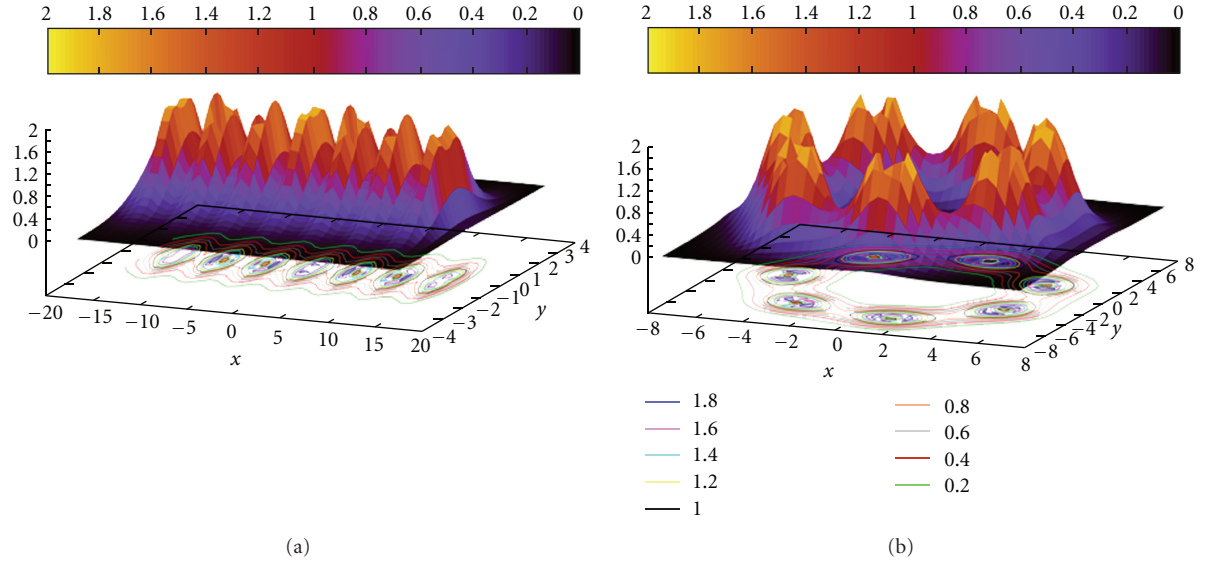

Figure 4: Charge density of the zigzag (7, 0) graphene (a) and nanotube (b).

a double-ζ singly polarized (DZP) basis set [17]. Basis sets of this size have been shown to yield structures and total energies in good agreement with those of standard plane-wave calculations [18]. Real-space integration was performed on a regular grid corresponding to a plane-wave cutoff around 300 Ry, for which the structural relaxations and the electronic energies are fully converged. For the total energy calculations of graphene and isolated CNTs we used 25 k points. We relaxed the isolated CNTs until the stress tensors were below 0,04 eV/Å^3 and calculated the theoretical lattice constant. In the band structure calculations we used 161 band k vectors for the A, Γ, M, K, Γ, and A points.

3. Results and Discussion

We first relaxed the zigzag (6, 0) and (7, 0), armchair (7, 7), and chiral (6, 2) and (6, 3) graphene and nanotubes. We considered their geometrical and electronic properties while selecting these structures. For graphene structure, we constituted the super cell structure by increasing atom number along the x-axis so that we could obtain the suitable nanotubes. Then, we rolled them into a cylindrical shape along the chiral vector of graphenes and created the nanotubes. Consequently, we calculated the band structure, DOS and the charge density of these structures.

3.1. Zigzag Carbon Nanotubes. In Figure 1(b) we show the band structure of an isolated (6, 0) nanotube. Also, Figure 1(a) contains the graphene electronic dispersion. The right part of both graphics is the density of state of graphene and nanotube. The supercell graphene and isolated (6, 0) nanotube include 24 carbon atoms. The maximum valence and minimum conduction bands are indicated by the black dots in the band structure figures.

We examine the electronic bands of graphene and nanotube along the high-symmetry A-Γ-M-K-Γ-A directions. The Femi level is set to zero in Figures 1(a) and 1(b) and other band structure graphics. The graphene is a semimetal, but the Fermi surface consists only of six distinct points. This peculiar Fermi surface is responsible, for example, for the sometimes metallic and sometimes semiconducting character of carbon nanotubes and also for effects like phonon softening in metallic tubes [7]. There are two carbon

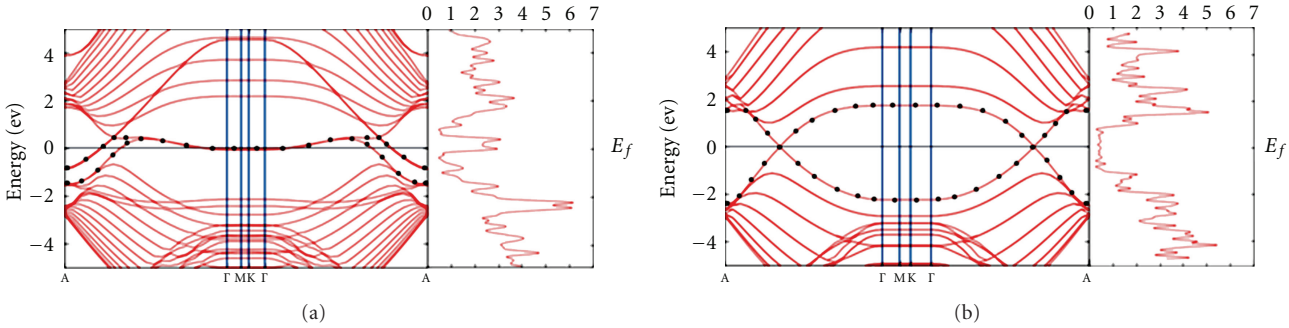

Figure 5: Electronic band structure and DOS of the armchair (7, 7) graphene (a) and nanotube (b).

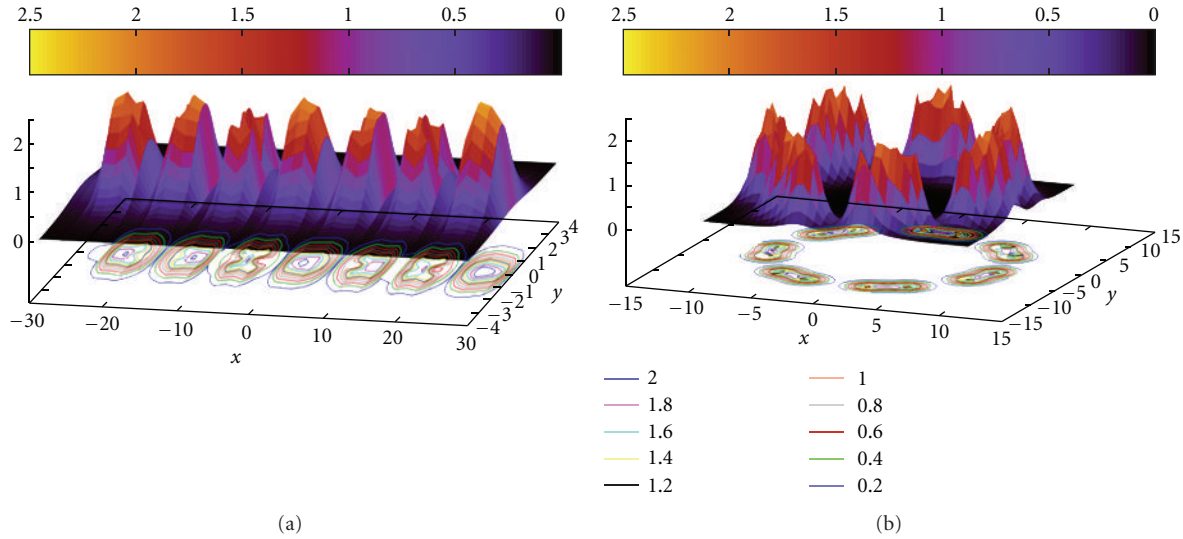

Figure 6: Charge density of the armchair (7, 7) graphene (a) and nanotube (b).

atoms in the unit cell of graphene. Along the x-axis, we increased the atom number of graphene up to 24 atoms and obtained a supercell graphene that has $\vec{C}_h = 14.8945$ Å. As a result of this process, the band structure of graphene shows similarities to the zigzag (6, 0) nanotube which has diameter = 4.74106 Å. Nevertheless, the electronic structure of the zigzag (6, 0) nanotube shows significant differences relative to (6, 0) graphene; for example, we see more intense bands near the Fermi level. The conduction band minimum that has energy −0.1556 eV is between the A-Γ points and close to the Γ point. The valence band maximum that has energy 0.4101 eV is between the K-Γ points and close to the Γ point. Thus, we can tell that the zigzag (6, 0) nanotube shows metallic behavior. In Figure 1, both the valence and conduction bands are affected by the rolling up of the graphene sheet. The conduction bands, however, are strongly affected by curvature of the nanotube [19].

To investigate the effect of rolling on the band structure of a nanotube, we realize a similar calculation for the zigzag (7, 0) nanotube. Figure 3 shows the band structure and DOS of the zigzag (7, 0) graphene (a) and nanotube (b). In the calculation of (7, 0) graphene and nanotube, we only changed the chiral vector of graphene along the x-axis. Thus, we obtained that the chiral vector of graphene is 17.3374 Å and the diameter of (7, 0) nanotube is 5.51868 Å. This difference did not affect too much the electronic structure of graphene except for the valence and conduction band number. The valence band number of the (6, 0) graphene and nanotube is 48 and that of the (7, 0) graphene and nanotube is 56. Band structure of the (7, 0) graphene is almost the same as that of the (6, 0) graphene. However, the electronic properties of (7, 0) nanotube significantly change. We have seen that the zigzag (7, 0) nanotube shows semiconducting properties. We found that the semiconducting energy gap is $E_g = 0.5022$ eV for this nanotube. Also, we can see the band gap change in the Fermi level by examining the DOS graphic.

3.2. Armchair Carbon Nanotubes. To research the effect of curvature on the band structure of SWCNTs, we show the same calculations for different graphenes in Figure 5(a). To obtain the armchair (7, 7) graphene, the $\vec{C}_h$ vector rotates 30° relative to the zigzag (7, 0).This chiral angle difference affects the structure of graphene band relative to a zigzag graphene. We obtained that the chiral vector of the (7, 7) graphene is 29.9179 Å and the diameter of the (7, 7) nanotube is 9.52316 Å. We show that the band gaps

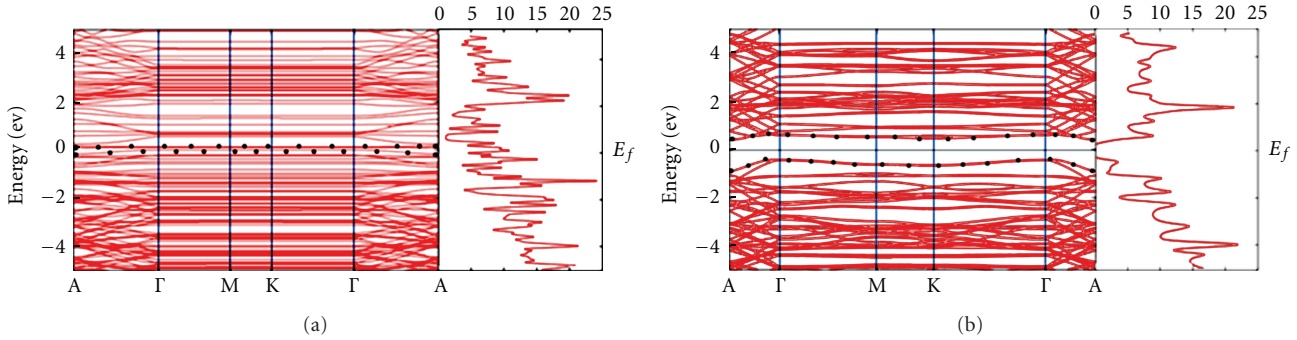

Figure 7: Electronic band structure and DOS of the chiral (6, 2) graphene (a) and nanotube (b).

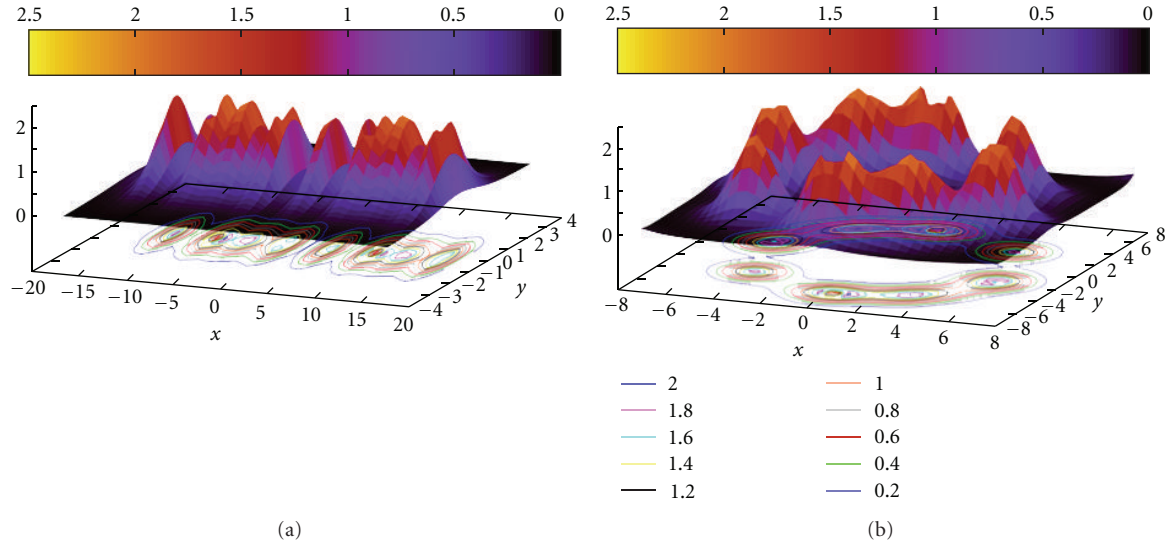

Figure 8: Charge density of the chiral (6, 2) graphene (a) and (6, 2) nanotube (b).

in the Γ-M-K-Γ points of (6, 0) and (7, 0) graphene are 0.5355 eV and 0.2275 eV, respectively. But, the armchair (7, 7) graphene does not have a similar band gap. Also, it clearly shows metallic properties. After constituting armchair (7, 7) nanotube, the tube k_z direction is now along the Γ-K-M line of graphene. The graphene Fermi point at K is thus always included in the allowed states of an armchair tube and these tubes have metallic properties [20].

In Figures 2(a), 4(a), and 6(a), because we generate a supercell graphene along the x-axis, the geometrical structures of these graphenes contain defects. So, the maximum valence band in the band structure of graphene exceeds the Fermi level. When we generate a nanotube by using supercell graphenes, these defects are eliminated.

3.3. Chiral Carbon Nanotubes. The electronic dispersion for the (6, 2) graphene and chiral (6, 2) nanotube is shown in Figures 7(a) and 7(b), respectively. We rotated the chiral angle of (6, 0) graphene by 13.89° to obtain the chiral (6, 2) nanotube. The graphene electronic dispersion is dramatically different according to the valence and conduction bands of the other graphenes. This difference in graphene shows itself in chiral (6, 2) nanotube as well. The conduction band minimum is at the A point energy of 0.0934 eV and the valence band minimum is at the Γ point energy of 0.0031 eV. We found that the (6, 2) graphene is semiconducting with low energy gap of 0.0965 eV. In addition, (6, 2) graphene does not have the defects that the other graphenes have. Then, when (6, 2) graphene sheet is rolled into a cylindrical shape, chiral (6, 2) nanotube is obtained, which shows different semiconducting behavior from the other nanotubes. Because, the band energy of A point is close to the band energy in other high symmetry points. The conduction band minimum has energy 0.4091 eV is at A point and the valence band maximum has energy −0.42 eV is at Γ point. The semiconducting energy gap of chiral (6, 2) nanotube is E_g = 0.8291 eV, and we can say that this nanotube has a big band gap relative to other nanotubes.

Finally, our last calculation is for the (6, 3) graphene and chiral (6, 3) nanotube, which is shown in Figures 9(a) and 9(b), respectively. These structures are similar with (6, 2). We only rotated the chiral angle of (6, 0) graphene by 19.11°. However, we have seen that this angle has a big effect on the electronic properties of the nanotube (6, 3). Firstly,

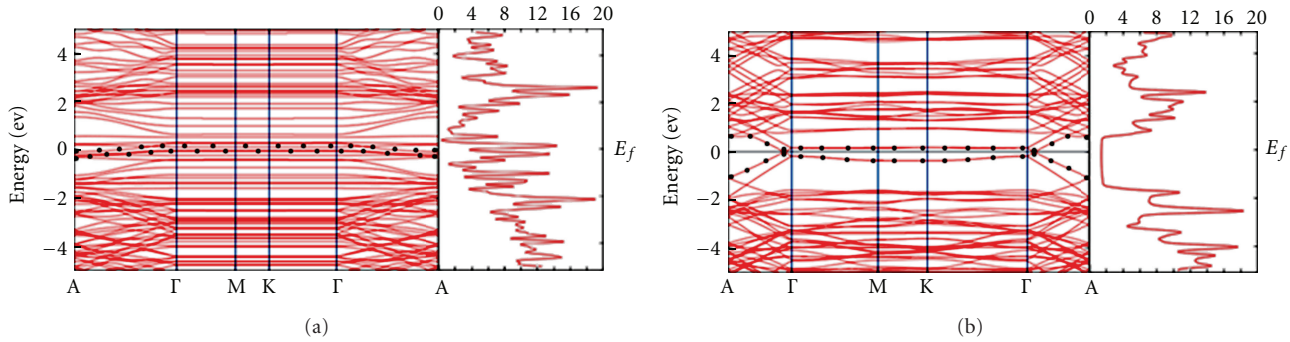

Figure 9: Electronic band structure and DOS of the chiral (6, 3) graphene (a) and nanotube (b).

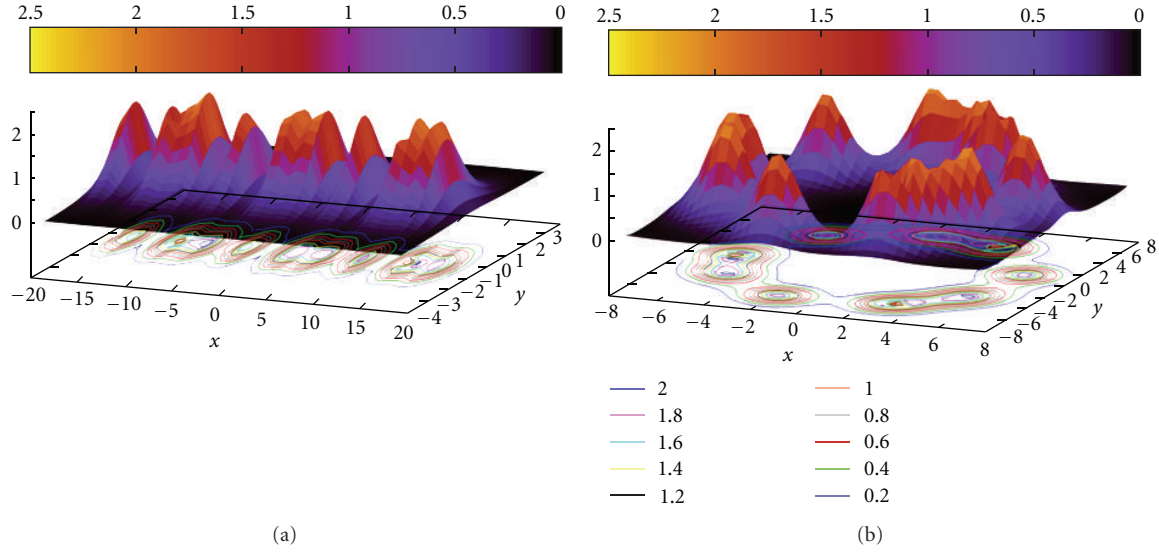

Figure 10: Charge density of the chiral (6, 3) graphene (a) and chiral (6, 3) nanotube (b).

if we examine the graphene band structure, we show that the graphene has indirect band gap with $E_g = 0.0516\,\text{eV}$. This band gap is smaller than that of the (6, 2) graphene. Moreover, (6, 3) graphene has a different band gap because of the geometrical structure defects. The conduction bands are strongly affected by these defects. When this graphene sheet is rolled into a cylindrical shape, we constitute chiral (6, 3) nanotube and can observe better changes in its electronic dispersion. We obtain a low band gap, $E_g = 0.0488\,\text{eV}$, for chiral (6, 3) nanotube, which is a quasimetallic nanotube. The lowest conduction band has energy 0.0237 eV, which is between the A-Γ points and close to the Γ point. The highest valence band has energy −0.0251 eV, which is between the A-Γ points and close to the Γ point. We show that the valence and conduction bands of nanotubes are asymmetric with respect to the Fermi level. There are two important reasons for the different behavior below and above the Fermi level. Firstly, the electronic dispersion of graphene is different for the valence and conduction bands. Secondly, higher bands move toward the Fermi level because of the curvature.

3.4. Charge Density of Carbon Nanotubes. In this study we obtained the self-consistent density by using eigenfunctions of the system in the k-points. The valence charge density for the calculated all nanotubes is presented in Figures 2, 4, 6, 8, and 10, respectively. All figures for charge density consist of the 2D contour lines and 3D surface in the XY plane. Charge density distribution provides information on the geometric structure and electronic properties of the graphene and nanotube in the figures which consist of the color gradient. The yellow, red, blue, and black colors indicate the electron density from higher to lower. The graphics of the nanotube and graphene have the minimum and maximum density. Maximum peaks represent the carbon atoms and the C–C bonds. In the minimum density regions, the carbon atoms do not bond with each other on the surface. We show the charge density for zigzag (6, 0) and (7, 0) graphene and nanotube in Figures 2 and 4, which contains six and seven peaks, respectively. These peaks have two little peaks. The little peaks represent the electrons that bond to other two carbon atoms because the graphene and nanotubes have

the sp2 hybridization. In Figure 6 we show the charge density of the armchair (7, 7) graphene (a) and nanotube (b). Here, there are 7 peaks and each peak contains two carbon atoms that bond to each peak. Armchair (7, 7) nanotube has lower charge density than zigzag nanotubes (peaks of nanotubes are the red color) because it has a big diameter with respect to zigzag nanotubes. The charge densities of the chiral graphene and nanotubes are seen in Figures 8 and 10. They have more electron density on the surface with respect to zigzag and armchair because of their geometrical structure. There are defects in the zigzag and armchair graphenes, but the chiral (6, 2) graphene does not have such defects because of more electron density in their surface. The chiral (6, 3) graphene has lower electron density relative to the chiral (6, 2) graphene. So we show the structural defects in the conduction band of the chiral (6, 3) graphene. We can say that these defects are caused by minimum density regions between carbon atoms.

4. Conclusions

We have reported the structural and electronic properties of the supercell graphene and SWCNTs, which consist of zigzag (6, 0), zigzag (7, 0), chiral (6, 2), chiral (6, 3), and armchair (7, 7), and investigated the effect of rolling for nanotubes. Moreover, we have examined the charge density of these structures. The zigzag and armchair supercell graphenes have structural defects because of the charge density dispersion on their surface. However, we found that chiral (6, 2) graphene does not have defects in the structure. When these graphene sheets are rolled into a cylindrical shape, the obtained nanotubes do not have defects.

While the zigzag (6, 0) nanotube shows metallic behavior, zigzag (7, 0) nanotube shows semiconducting behavior and we found that its band gap is of $E_g = 0.5022\,\text{eV}$. The armchair (7, 7) nanotube shows similar properties to those of armchair (7, 7) graphene and shows metallic behavior. For chiral (6, 2) graphene, we obtain a low band gap of $E_g = 0.0965\,\text{eV}$. Chiral (6, 2) nanotube shows semiconducting behavior and has a big band gap of $E_g = 0.8291\,\text{eV}$. A similar way to chiral (6, 2) graphene for chiral (6, 3) graphene, we obtained a low band gap is $E_g = 0.0516\,\text{eV}$. When this graphene is transformed to chiral (6, 3) nanotube, we obtain the quasimetallic chiral (6, 3) nanotube whose band gap is of $E_g = 0.0488\,\text{eV}$.

References

[1] S. Iijima, "Helical microtubules of graphitic carbon," *Nature*, vol. 354, no. 6348, pp. 56–58, 1991.

[2] N. Hamada, S. I. Sawada, and A. Oshiyama, "New one-dimensional conductors: graphitic microtubules," *Physical Review Letters*, vol. 68, no. 10, pp. 1579–1581, 1992.

[3] R. Saito, M. Fujita, G. Dresselhaus, and M. S. Dresselhaus, "Electronic structure of chiral graphene tubules," *Applied Physics Letters*, vol. 60, no. 18, pp. 2204–2206, 1992.

[4] J. W. Mintmire, B. I. Dunlap, and C. T. White, "Are fullerene tubules metallic?" *Physical Review Letters*, vol. 68, no. 5, pp. 631–634, 1992.

[5] R. Saito, M. Fujita, G. Dresselhaus, and M. S. Dresselhaus, "Electronic structure of graphene tubules based on C_{60}," *Physical Review B*, vol. 46, no. 3, pp. 1804–1811, 1992.

[6] G. Dresselhaus, M. S. Dresselhaus, and P. C. Eklund, *Science of Fullerenes and Carbon Nanotubes*, Academic Press, San Diego, Calif, USA, 1996.

[7] R. Saito, M. Fujita, G. Dresselhaus, and M. S. Dresselhaus, *Physical Properties of Carbon Nanotubes*, Imperial College Press, London, UK, 6th edition, 2007.

[8] C. Journet, W. K. Maser, P. Bernier et al., "Large-scale production of single-walled carbon nanotubes by the electric-arc technique," *Nature*, vol. 388, no. 6644, pp. 756–758, 1997.

[9] C. Dekker, S. J. Tans, M. H. Devoret et al., "Molecular nanostructures," in *Proceedings of the Winter School on Electronic Properties of Novel Materials*, H. Kuzmany, J. Fink, M. Mehring, and S. Roth, Eds., Springer, New York, NY, USA, 1997.

[10] E. D. Minot, Y. Yaish, V. Sazonova, J. Y. Park, M. Brink, and P. L. McEuen, "Tuning carbon nanotube band gaps with strain," *Physical Review Letters*, vol. 90, no. 15, article 156401, 4 pages, 2003.

[11] S. Dohn, J. Kjelstrup-Hansen, D. N. Madsen, K. Mølhave, and P. Bøggild, "Multi-walled carbon nanotubes integrated in microcantilevers for application of tensile strain," *Ultramicroscopy*, vol. 105, no. 1–4, pp. 209–214, 2005.

[12] T. W. Tombler, C. Zhou, L. Alexseyev et al., "Reversible electromechanical characteristics of carbon nanotubes under local-probe manipulation," *Nature*, vol. 405, no. 6788, pp. 769–772, 2000.

[13] J. T. Frey and D. J. Doren, *TubeGen 3.2*, University of Delaware, Newark, Del, USA, 2003.

[14] D. Sánchez-Portal, P. Ordejón, E. Artacho, and J. M. Soler, "Density-functional method for very large systems with LCAO basis sets," *International Journal of Quantum Chemistry*, vol. 65, no. 5, pp. 453–461, 1997.

[15] J. P. Perdew and A. Zunger, "Self-interaction correction to density-functional approximations for many-electron systems," *Physical Review B*, vol. 23, no. 10, pp. 5048–5079, 1981.

[16] N. Troullier and J. L. Martins, "Efficient pseudopotentials for plane-wave calculations," *Physical Review B*, vol. 43, no. 3, pp. 1993–2006, 1991.

[17] E. Artacho, D. Sánchez-Portal, P. Ordejón, A. García, and J. M. Soler, "Linear-scaling ab-initio calculations for large and complex systems," *Physica Status Solidi B*, vol. 215, no. 1, pp. 809–817, 1999.

[18] J. Junquera, Ó. Paz, D. Sánchez-Portal, and E. Artacho, "Numerical atomic orbitals for linear-scaling calculations," *Physical Review B*, vol. 64, no. 23, article 235111, 9 pages, 2001.

[19] X. Blase, L. X. Benedict, E. L. Shirley, and S. G. Louie, "Hybridization effects and metallicity in small radius carbon nanotubes," *Physical Review Letters*, vol. 72, no. 12, pp. 1878–1881, 1994.

[20] J. W. Mintmire and C. T. White, "Universal density of states for carbon nanotubes," *Physical Review Letters*, vol. 81, no. 12, pp. 2506–2509, 1998.